ELSEVIER

International Journal of Solids and Structures 41 (2004) 5903–5919

INTERNATIONAL JOURNAL OF SOLIDS and STRUCTURES

www.elsevier.com/locate/ijsolstr

Investigations of shear banding in an anisotropic hypoplastic material

Erich Bauer [a,b,c,*], Wenxiong Huang [a,b,c], Wei Wu [a,b,c]

[a] *Institute of General Mechanics, Graz University of Technology, Technikerstrasse 4 II, Graz A 8010, Austria*
[b] *Department of Civil, Surveying & Environmental Engineering, The University of Newcastle, Australia*
[c] *Institute of Geotechnical Engineering, University of Natural Resources & Applied Life Sciences, Vienna, Austria*

Received 28 April 2004
Available online 3 July 2004

Abstract

This paper focuses on the analysis of shear band formation in a cohesionless and initially transversely isotropic granular material based on a hypoplastic continuum approach. The constitutive equation for the evolution of the stress is formulated with a non-linear tensor-valued function depending on the current void ratio, the Cauchy stress, the rate of deformation and a structure tensor for anisotropy effects. The possibility of shear band formation in biaxial, plane strain compression is analyzed and the sensitivity of the shear band orientation to the slenderness of the specimen is discussed.

Keywords: Anisotropy; Hypoplasticity; Granular materials; Shear band

1. Introduction

In natural sand deposits an initially transverse isotropy can be explained by a preferred orientation of the long axis of non-spherical particles as a result of the sedimentation process (e.g. Oda et al., 1985). The plane perpendicular to the deposit direction is called bedding plane and it is a plane of isotropy. Experimental studies with sand specimens show that the orientation of the bedding plane relative to the principal stress directions has a significant influence on the stress-strain behavior (e.g. Arthur and Phillips, 1975; Lam and Tatsuoka, 1988; Tatsuoka et al., 1990). The stiffness and the peak friction angle are higher for loading perpendicular to the bedding plane than for loading parallel to it. They are also influenced by the mean pressure and the current density. However, for large monotonic shearing the stress ratio approaches a stationary value, which seems to be independent of the bedding plane (e.g. Yamada and Ishihara, 1979).

* Corresponding author. Present address: Institute of General Mechanics, Graz University of Technology, Technikerstrasse 4 II, Graz A 8010, Austria. Tel.: +43-316-8737148; fax: +43-316-8737641.
E-mail address: erich.bauer@tugraz.at (E. Bauer).

0020-7683/$ - see front matter © 2004 Elsevier Ltd. All rights reserved.
doi:10.1016/j.ijsolstr.2004.05.052

This indicates that under large shearing the initial anisotropy declines as a result of grain rotations and grain rearrangements and it may be swept out when the granular material reaches a critical state (e.g. see Fig. 13 in Lam and Tatsuoka, 1988). In order to model such a behavior a unified description of the interaction between the loading history, the mean pressure, the density and the parameters of anisotropy is necessary.

The focus of the paper is on modeling the mechanical behavior of an initially transverse isotropy in dry and cohesionless granular materials using a continuum approach. For this purpose a particular hypoplastic constitutive model by Gudehus (1996) and Bauer (1996) for a cohesionless and initially isotropic material was extended with respect to transverse isotropy. The extended hypoplastic model takes into account the current void ratio, the Cauchy stress tensor, the rate of deformation, and a structure tensor which is defined by the dyadic product of the director vector of the plane of isotropy. In order to model non-linear and inelastic material behavior the evolution equation for the stress tensor consists of the sum of a tensor function which is linear in the rate of deformation and a tensor function which is non-linear in the rate of deformation according to the concept of hypoplasticity (Kolymbas, 1985, 1991). In this sense the hypoplastic model can be assigned to a class of constitutive models referred to as incrementally non-linear models (Darve, 1974, 1991; Chambon, 1989). Critical states are included in the hypoplastic concept for a simultaneous vanishing of the stress rate and the volume strain rate under monotonic shearing (Wu and Bauer, 1992; Bauer, 1995; Wu et al., 1996). Transversely isotropic material properties are included with a certain invariant form of a tensor function given by Boehler and Sawczuk (1977). The tensor function depends on the stress tensor and on a second order structure tensor and it is incorporated in the non-linear part of the constitutive equation according to the concept proposed by Wu (1998). While the coefficients of anisotropy are assumed to be constant in the earlier version by Wu (1998), an evolution of anisotropy depending on the relative density is considered in the present version. It is assumed that the influence of the initial anisotropy decreases for large shearing and it is swept out in critical-states (Bauer and Huang, 1999).

The paper is organized as follows. In Section 2.1 the concept of hypoplasticity is briefly outlined for an initially isotropic material behavior. Section 2.2 describes the specific form of the evolution equation of the stress tensor given by Gudehus (1996) and Bauer (1996). Herein the influence of the mean pressure and the void ratio on the incremental stiffness for an initially isotropic material is taken into account with a single set of constants. Following Wu (1998) Section 2.3 deals with the extension of the model by Gudehus and Bauer with respect to initially transversely isotropic material properties and demonstrates the performance of the model for homogeneous deformations and for constant parameters of anisotropy. In Section 2.4 an evolution equation for the parameters of anisotropy is presented according to the proposal by Bauer and Huang (1999). In Section 3 the influence of the orientation of the bedding plane on the formation of shear bands under plane strain compression is studied. In particular the possibility of a spontaneous shear band formation of a material element is analyzed for different bedding angles (Section 3.1). Attention is paid to the lowest stress ratio where a shear band bifurcation is possible. Moreover, the influence of the initial void ratio and the bedding angle on the bifurcation stress and the corresponding shear band inclination is studied. In Section 3.2 the sensitivity of the shear band orientation to the slenderness of an initially rectangular specimen is investigated for both an initially homogeneous void ratio and an initially probabilistic void ratio distribution. Concluding remarks are finally made in Section 4.

Throughout the paper compression stresses and strains are defined as negative. Bold lower case, bold upper case and calligraphic letters denote vectors, tensors of second order and of fourth order, respectively. In particular, the identity tensor of second order is denoted by $\mathbf{I}$ and the identity tensor of fourth order is denoted by $\mathscr{I}$. For vector and tensor components indices notation with respect to a rectangular Cartesian basis $\mathbf{e}_i$ $(i = 1, 2, 3)$ is used. Operations and symbols are defined as: $\mathbf{ab} = a_i b_i$, $\mathbf{Ab} = A_{ij} b_j \mathbf{e}_i$, $\mathbf{a} \otimes \mathbf{b} = a_i b_j \mathbf{e}_i \otimes \mathbf{e}_j$, $\mathbf{I} = \delta_{ij} \mathbf{e}_i \otimes \mathbf{e}_j$, $\mathscr{I} = \mathbf{I} \odot \mathbf{I} = \delta_{ik}\delta_{jl} \mathbf{e}_i \otimes \mathbf{e}_j \otimes \mathbf{e}_k \otimes \mathbf{e}_l$, $\mathbf{A} \odot \mathbf{B} = A_{ik} B_{jl} \mathbf{e}_i \otimes \mathbf{e}_j \otimes \mathbf{e}_k \otimes \mathbf{e}_l$, $\mathbf{A} \otimes \mathbf{B} = A_{ij} B_{kl} \mathbf{e}_i \otimes \mathbf{e}_j \otimes \mathbf{e}_k \otimes \mathbf{e}_l$, $\mathbf{AB} = A_{ik} B_{kj} \mathbf{e}_i \otimes \mathbf{e}_j$, $\mathscr{A} : \mathbf{B} = A_{ijkl} B_{kl} \mathbf{e}_i \otimes \mathbf{e}_j$ and $\mathbf{I} : \mathbf{A} = A_{ii}$. Herein δ_{ik} denotes

the Kronecker delta and the summation convention over repeated indices is employed. A superimposed dot indicates a time derivative, i.e. $\dot{\mathbf{A}} = \mathrm{d}\mathbf{A}/\mathrm{d}t$, and the symbol $[[\mathbf{A}]]$ denotes the jump of the field quantity $\mathbf{A}$ immediately on the plus side and on the minus side of a discontinuity, i.e. $[[\mathbf{A}]] = \mathbf{A}^{+} - \mathbf{A}^{-}$.

2. The hypoplastic constitutive model

2.1. Inelastic material properties

In hypoplasticity inelastic material properties are modeled with a constitutive equation of the rate type where the objective stress rate $\overset{\circ}{\mathbf{T}}$ is expressed by an isotropic tensor-valued function consisting of the sum of the tensor function $\mathscr{A} : \mathbf{D}$, which is linear in the rate of deformation $\mathbf{D}$, and the tensor function $\mathbf{B}\sqrt{\mathbf{D} : \mathbf{D}}$, which is non-linear in $\mathbf{D}$, i.e.

$$\overset{\circ}{\mathbf{T}} = \mathscr{A} : \mathbf{D} + \mathbf{B}\sqrt{\mathbf{D} : \mathbf{D}}. \tag{1}$$

Herein the fourth order tensor $\mathscr{A}$ and the second order tensor $\mathbf{B}$ are functions of the current Cauchy stress tensor $\mathbf{T}$ and may also depend on additional state quantities such as the current void ratio e (e.g. Wu and Bauer, 1992; Bauer and Wu, 1994). The constitutive equation (1) is positively homogeneous of the first order in $\mathbf{D}$, thus the material behavior to be described is rate independent. Depending on the specific representation of tensor $\mathscr{A}$ the function $\mathscr{A} : \mathbf{D}$ describes a hyperelastic or hypoelastic material in the sense of Truesdell (1955). Together with the non-linear team of $\mathbf{B}\sqrt{\mathbf{D} : \mathbf{D}}$ in $\mathbf{D}$ an inelastic material behavior is modeled in hypoplasticity with a single constitutive equation and there is no need to distinguish between elastic and plastic parts of the deformation (Kolymbas, 1985, 1991). Limit states are included in the constitutive equation (1) for a vanishing stress rate, i.e. for states with $\mathscr{A} : \mathbf{D} = -\mathbf{B}\sqrt{\mathbf{D} : \mathbf{D}}$. Specific representations of the tensor functions $\mathscr{A}$ and $\mathbf{B}$ have to fulfill several conditions which are related to general principals of rational continuum mechanics and to the mechanical behaviour of granular materials observed in experiments (e.g. Wu and Kolymbas, 1990; Gudehus, 1996; Bauer, 1996). A comprehensive overview of the procedures followed in finding appropriate functions can be found, for instance, in Wu and Kolymbas (2000) and Bauer and Herle (2000).

2.2. Pressure and density dependent properties of inherently isotropic materials

The mechanical behavior of cohesionless frictional materials like sand is strongly influenced by the pressure level and the current density. In order to model such properties the following specific representation of Eq. (1) for an inherently isotropic material is considered (Gudehus, 1996; Bauer, 1996):

$$\overset{\circ}{\mathbf{T}} = f_s(e,p)[\mathscr{L}(\hat{\mathbf{T}}) : \mathbf{D} + f_d(e,p)\mathbf{N}(\hat{\mathbf{T}})\sqrt{\mathbf{D} : \mathbf{D}}], \tag{2}$$

with

$$\mathscr{L}(\hat{\mathbf{T}}) = \hat{a}^2\mathscr{I} + \hat{\mathbf{T}} \otimes \hat{\mathbf{T}}, \tag{3}$$

and

$$\mathbf{N}(\hat{\mathbf{T}}) = \hat{a}(\hat{\mathbf{T}} + \hat{\mathbf{T}}^{*}). \tag{4}$$

Herein the tensors $\mathscr{L}(\hat{\mathbf{T}})$ and $\mathbf{N}(\hat{\mathbf{T}})$ are functions of the normalized stress tensor $\hat{\mathbf{T}} = \mathbf{T}/(\mathbf{I} : \mathbf{T})$ and the deviatoric part $\hat{\mathbf{T}}^{*} = \hat{\mathbf{T}} - \mathbf{I}/3$. Factor $\hat{a}$ in Eqs. (3) and (4) depends on the normalized stress deviator $\hat{\mathbf{T}}^{*}$ and the critical friction angle φ:

$$\hat{a} = \frac{\sin\varphi}{3-\sin\varphi}\left[\sqrt{\frac{(8/3) - 3(\hat{\mathbf{T}}^* : \hat{\mathbf{T}}^*) + \sqrt{3/2}(\hat{\mathbf{T}}^* : \hat{\mathbf{T}}^*)^{3/2}\cos(3\theta)}{1 + \sqrt{3/2}(\hat{\mathbf{T}}^* : \hat{\mathbf{T}}^*)^{1/2}\cos(3\theta)}} - \sqrt{\hat{\mathbf{T}}^* : \hat{\mathbf{T}}^*}\right], \tag{5}$$

with the Lode-angle θ, which is defined as

$$\cos(3\theta) = -\sqrt{6}\frac{\mathbf{I} : \hat{\mathbf{T}}^{*3}}{[\mathbf{I} : \hat{\mathbf{T}}^{*2}]^{3/2}}.$$

For critical states, which are defined for a stationary stress $\mathbf{T}_c$ and stationary void ratio e_c under a fixed strain rate $\mathbf{D}_c \neq \mathbf{0}$, factor $\hat{a}$ is equal to the Euclidean norm of the normalized stress deviator, i.e.

$$\hat{a}(\hat{\mathbf{T}}_c^*) = \hat{a}_c = \sqrt{\hat{\mathbf{T}}_c^* : \hat{\mathbf{T}}_c^*}. \tag{6}$$

In particular, for critical states, relation $\hat{a}$ in (5) represents the stress limit condition given by Matsuoka and Nakai (1977) as shown in Fig. 1a. It can be proved that for monotonic shearing the limit stress states given by relation (6) will asymptotically be reached independent of the initial void ratio and stress state (Bauer, 2000). The influence of the mean pressure $p = -\mathbf{I} : \mathbf{T}/3$ and the current void ratio e on the response of the constitutive equation (2) is taken into account by the density factor f_d, i.e.

$$f_d = \left(\frac{e - e_d}{e_c - e_d}\right)^{\alpha}, \tag{7}$$

and the stiffness factor f_s, i.e.

$$f_s = \left(\frac{e_i}{e}\right)^{\beta}\frac{1+e_i}{e_i}\frac{h_s}{nh_i(\hat{\mathbf{T}} : \hat{\mathbf{T}})}\left(\frac{3p}{h_s}\right)^{1-n}, \tag{8}$$

with

$$h_i = \frac{8\sin^2\varphi}{(3-\sin\varphi)^2} + 1 - \frac{2\sqrt{2}\sin\varphi}{3-\sin\varphi}\left(\frac{e_{io} - e_{do}}{e_{co} - e_{do}}\right)^{\alpha}.$$

Herein $\alpha < 0.5$ and $\beta > 1$ are constitutive constants. In particular factor f_d models the dilatancy behavior and the maximum stress ratio while factor f_s models the influence of the stress and density on the incremental stiffness. In relations (7) and (8) the maximum void ratio e_i, the minimum void ratio e_d and the critical void ratio e_c are pressure dependent according to

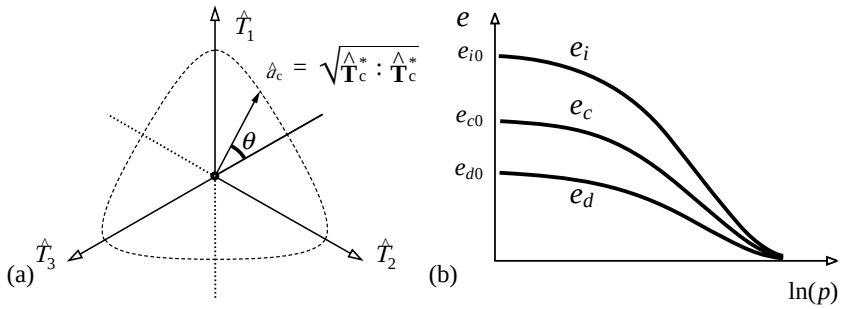

Fig. 1. (a) Contour of the stress limit condition in the deviator-plane, (b) decrease of the maximum void ratio e_i, the critical void ratio e_c and the minimum void ratio e_d with increasing mean pressure p.

$$\frac{e_i}{e_{io}} = \frac{e_d}{e_{do}} = \frac{e_c}{e_{co}} = \exp\left[-\left(\frac{3p}{h_s}\right)^n\right], \tag{9}$$

where e_{io}, e_{do} and e_{co} are the corresponding values for $p \approx 0$ as shown in Fig. 1b. In relation (9) the parameter h_s with the dimension of stress scales the mean pressure p while the dimensionless exponent n reflects the degradation of the limit void ratios and the critical void ratio with increasing pressure. It is obvious that with relation (9) the density factor f_d also depends on the mean pressure p with the exception of states where the current void ratio is equal to the critical one. In this case the function of f_d becomes equal to one, which is independent of the magnitude of the mean pressure. This property of the density factor plays an important role for a consistent modeling of critical states (Bauer, 1995, 2000). For the evolution of the current void ratio e the assumption is made that the volume change of grains can be neglected. To this end, the rate of the void ratio can be directly derived from the mass balance, which yields

$$\dot{e} = (1+e)\mathbf{I} : \mathbf{D}. \tag{10}$$

Altogether the hypoplastic model for an initially isotropic material behavior includes eight constants. The following values $\varphi = 30°$, $h_s = 190$ MPa, $n = 0.4$, $e_{io} = 1.20$, $e_{co} = 0.82$, $e_{do} = 0.51$, $\alpha = 0.14$, $\beta = 1.05$ are adapted to a medium quartz sand and used for the numerical calculations in the present paper. Details about the calibration procedure can be found for instance in Bauer (1996) and Herle and Gudehus (1999).

2.3. Initially transversely isotropic material

In order to take into account anisotropic properties, the state variables of the hypoplastic constitutive model are extended with a structure tensor $\mathbf{S} = \mathbf{s} \otimes \mathbf{s}$ represented by the dyadic product of the normal vector $\mathbf{s}$ of the isotropic plane or so-called bedding plane (Fig. 2). It was proposed by Wu (1998) to incorporate the structure tensor $\mathbf{S}$ in the non-linear part of the constitutive equation for the stress rate by a linear transformation of tensor $\mathbf{N}(\hat{\mathbf{T}})$ with a fourth order tensor $\mathscr{P}(\mathbf{S})$. Thus, the extended evolution equation for the stress tensor reads

$$\overset{\circ}{\mathbf{T}} = f_s(e,p)\left[\mathscr{L}(\hat{\mathbf{T}}) : \mathbf{D} + f_d(e,p)\mathscr{P}(\mathbf{S}) : \mathbf{N}(\hat{\mathbf{T}})\sqrt{\mathbf{D} : \mathbf{D}}\right], \tag{11}$$

with

$$\mathscr{P}(\mathbf{S}) = (\eta_1 + \eta_3 - 2\eta_2)(\mathbf{S} \otimes \mathbf{S}) + \eta_3 \mathscr{I} + (\eta_2 - \eta_3)(\mathbf{S} \odot \mathbf{I} + \mathbf{I} \odot \mathbf{S}). \tag{12}$$

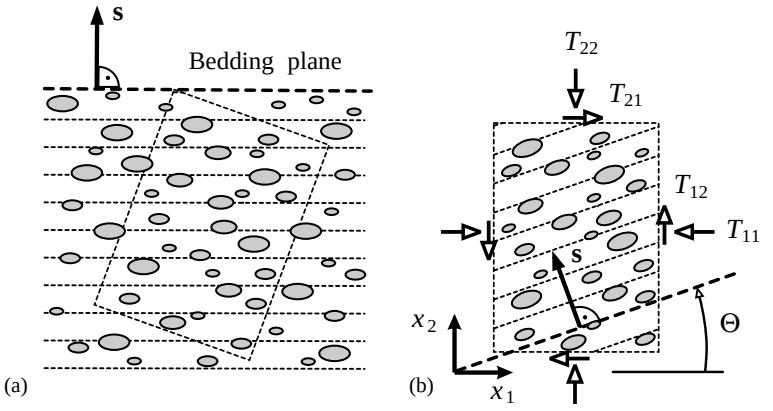

Fig. 2. Normal vector $\mathbf{s}$ of the isotropic plane (bedding plane): (a) orientation of the bedding plane during sedimentation, (b) stress components T_{ij} and inclination angle Θ of the bedding plane with respect to a fixed Cartesian co-ordinate system.

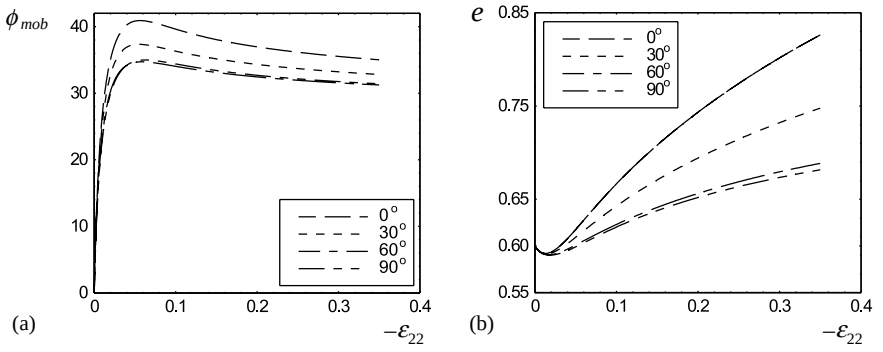

Fig. 3. Triaxial compression under a constant lateral stress of $T_{11} = -100$ kPa, an initial void ratio of $e_0 = 0.6$, for constant parameters of anisotropy and for bedding angles of $\Theta = 0°, 30°, 60°, 90°$: (a) mobilized friction angle ϕ_{mob} against vertical strain ε_{22}, (b) evolution of the void ratio e against vertical strain ε_{22}.

Herein η_i $(i = 1, 2, 3)$ are material parameters. It should be noted that the choice of representation (12) is motivated by a similar form originally proposed by Boehler and Sawczuk (1977) to describe the plastic behavior of a transversely isotropic material. Anisotropy is more pronounced for $\eta_i < 1$ and vanishes for $\eta_i = 1$. For the latter case the tensor function $\mathscr{P}(\mathbf{S})$ in Eq. (12) reduces to $\mathscr{I}$ and the constitutive relation (2) for an initially isotropic material is recovered.

For $\eta_1 = 0.8805$, $\eta_2 = 0.9764$ and $\eta_3 = 1.0$ the response of the constitutive model for triaxial compression under constant lateral pressure of $T_{11} = -100$ kPa and an initial void ratio of $e_0 = 0.6$ is shown for different bedding angles in Fig. 3. The peak friction angle $\phi_P = \max(\phi_{\text{mob}})$ is higher and the dilatancy is more pronounced for lower bedding angles. After the peak the mobilized friction angle $\phi_{\text{mob}} = \arcsin[(T_{22} - T_{11})/(T_{22} + T_{11})]$ slightly decreases and tends towards a stationary value.

2.4. Evolution equation for the parameters of anisotropy

It is obvious that with the constitutive equation (11) and for $\eta_i \neq 1$ the stress limit condition (6) is no longer met for an initially transverse isotropic material, i.e. the limit stress ratio is influenced by the orientation $\mathbf{s}$ of the isotropic plane as it was also discussed by Wu (1998). However, the experimental investigations by Yamada and Ishihara (1979) and Lam and Tatsuoka (1988) with initially transverse isotropic sand specimens show that for large monotonic shearing the stress ratio is independent of the initial orientation of the bedding plane. This indicates that under large shearing the initial anisotropy diminishes and may be swept out when the material reaches a stationary state. In order to reproduce the experimental findings an evolution of η_i corresponding to the evolution of the density factor f_d was proposed by Bauer and Huang (1999). Herein a degradation of the effect of the initial anisotropy is motivated by the experimental finding that under shearing accompanied by dilatancy, a reorientation of particles and consequently a reorientation of the direction of the contact planes takes place. Therefore, a relation between the evolution of dilatancy and the evolution of the parameter of anisotropy seems to be appropriate. Specifically, the rate of η_i is assumed to be proportional to the rate of f_d, i.e.

$$\dot{\eta}_i = \eta_{i0}\eta_i\dot{f}_d, \tag{13}$$

where η_{i0} $(i = 1, 2, 3)$ are constitutive constants. The integration of Eq. (13) with respect to the condition $\eta_i(f_d = 1) = 1$ leads to

$$\eta_i = \exp[\eta_{i0}(f_d - 1)]. \tag{14}$$

Thus, the quantities of η_i are directly related to the value of the density factor f_d given in Eq. (7). It is easy to prove that for $e = e_c$ the density factor and the parameters of anisotropy become $f_d = \eta_i = 1$. For such a critical state the corresponding critical void ratio and the critical stress ratio are independent of the initial anisotropy and the initial void ratio. Therefore, the stress limit condition (6) is also met for the extended constitutive equation (11) if the evolution equation (13) for the parameters of anisotropy is taken into account.

Based on the improved model the prediction for triaxial compression under a constant lateral stress of $T_{11} = -100$ kPa, an initial void ratio of $e_0 = 0.6$, and the parameters $\eta_{10} = 0.8$, $\eta_{20} = 0.15$ and $\eta_{30} = 0$ is shown for different bedding angles in Figs. 4 and 5. In contrast to the results in Fig. 3 the stationary value of the mobilized friction angle is now independent of the initial anisotropy. Consequently, for stationary states the stress limit condition (6) is also met for the case of an initially transverse isotropy. With the present hypoplastic model the peak friction angle depends on both the orientation of the bedding plane and on the density factor f_d. The influence of the initial void ratio e_0 and the bedding angle Θ on the peak friction angle $\phi_P = \max(\phi_{\text{mob}})$ is shown in Fig. 5. The peak friction angle is higher for $\Theta = 0°$. The influence of the orientation of the bedding plane is more pronounced for an initially lower void ratio. In accordance with

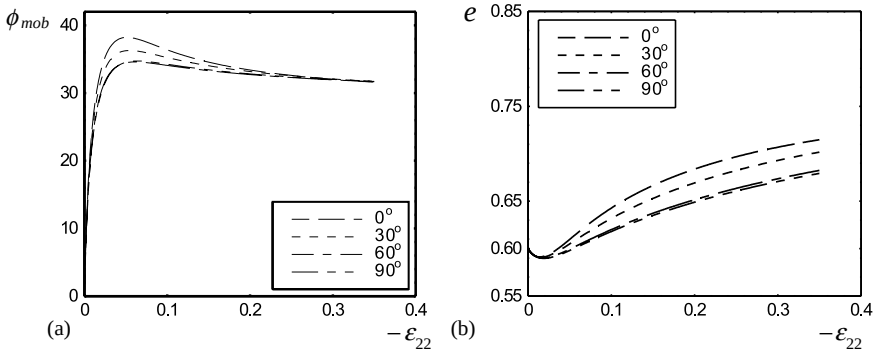

Fig. 4. Triaxial compression under a constant lateral stress of $T_{11} = -100$ kPa, an initial void ratio of $e_0 = 0.6$ and for bedding angles of $\Theta = 0°$, 30°, 60°, 90°: (a) mobilized friction angle ϕ_{mob} against vertical strain ε_{22}, (b) evolution of the void ratio e against vertical strain ε_{22}.

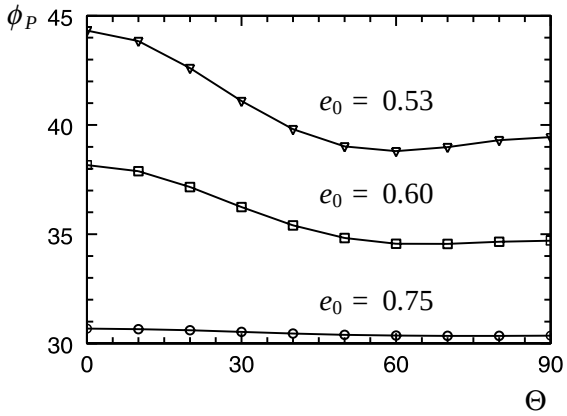

Fig. 5. Peak friction angle ϕ_P against the bedding angles Θ for different initial void ratios e_0.

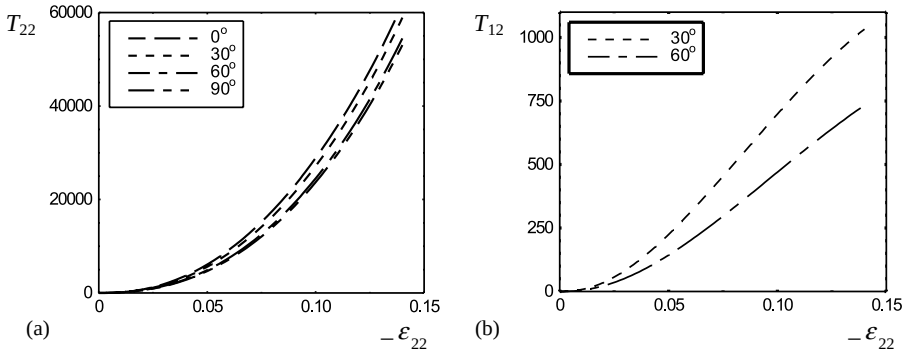

Fig. 6. Oedometric compression starting from an initially isotropic stress state of $T_0 = -1$ kPa and a void ratio of $e_0 = 0.53$: (a) vertical stress T_{22} against the vertical strain ε_{22}, (b) shear stress T_{12} against the vertical strain ε_{22}.

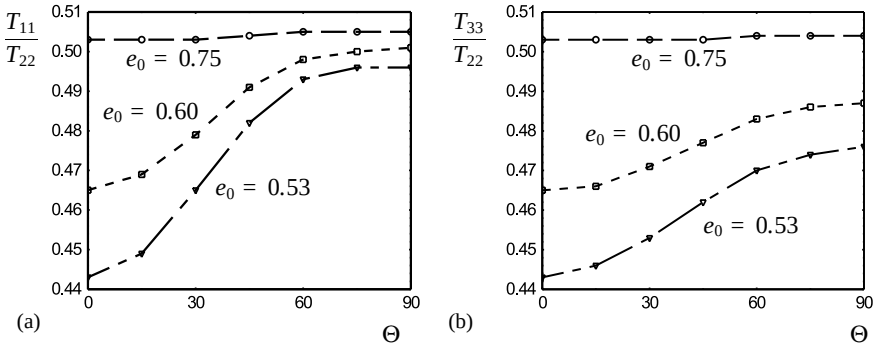

Fig. 7. Oedometric compression starting from an initially isotropic stress state of $T_0 = -1$ kPa and different initial void ratios e_0: (a) stress ratio T_{11}/T_{22} against the bedding angle Θ, (b) stress ratio T_{33}/T_{22} against the bedding angle Θ.

the experimental results (e.g. Lam and Tatsuoka, 1988) the peak friction angle becomes a minimum for $\Theta \approx 60°$.

The influence of the orientation of the bedding plane on the behavior under oedometric compression is shown in Fig. 6. For all calculations an initially isotropic stress state of $T_0 = -1$ kPa and a void ratio of $e_0 = 0.53$ was assumed. The stress–strain relation is non-linear and the magnitude of the vertical stress T_{22} increases faster for a lower bedding angle (Fig. 6a). Shear stresses $T_{12} = T_{21}$ occur as a result of the strain controlled test with the exception of bedding angles of $\Theta = 0°$ and $\Theta = 90°$ (Fig. 6b). The shear stress is about sixty times less than the normal stress. The lateral normal stresses T_{11} and T_{33} are only equal for $\Theta = 0°$. As shown in Fig. 7 the stress ratios T_{11}/T_{22} and T_{33}/T_{22} increase with an increase of the bedding angle and the changes are more pronounced for lower void ratios.

3. Investigation of the formation of shear bands

In this section the influence of the orientation of the bedding plane on the formation of shear bands under plane strain compression is studied. The possibility of a spontaneous shear band formation is investigated based on the general bifurcation theory given by Hill (1962), Rudnicki and Rice (1975) and Rice and Rudnicki (1980). The bifurcation condition is derived in a way similar to the ones outlined for

isotropic hypoplastic material models in earlier publications (e.g. Chambon and Desrues, 1985; Chambon, 1989; Wu and Sikora, 1991, 1992; Charlier et al., 1991; Bauer, 1999; Wu, 2000; Desrues and Chambon, 2002; Bauer et al., 2003). A comprehensive historical review of the individual contributions can be found for instance in Tamagnini et al. (2000, 2001). In order to investigate the sensitivity of the shear band orientation to the slenderness of the specimen the hypoplastic constitutive model was implemented in the commercial finite element program *Abaqus* as outlined by Huang (2000). A four-noded quadrilateral element for plane strain conditions with bilinear interpolation for the displacements is used. To alleviate the phenomenon of so-called volumetric locking a selective reduced integration technique is applied (Nagtegaal et al., 1974). The geometric non-linearity is taken into account using an updated Lagrangian formulation. The global equilibrium is formulated on the basis of the principle of virtual power and the non-linear equation system is solved by the Newton–Raphson iteration method. For the time integration of the constitutive equations a sub-stepping algorithm (Roddeman, 1997) is applied.

3.1. Bifurcation analysis

In the following the possibility of a spontaneous formation of a shear band is studied for a certain state $(\mathbf{T}, e)$ and a certain bedding angle Θ with respect to a fixed Cartesian co-ordinate system as sketched in Fig. 8. The shear plane or so-called discontinuity plane is characterized by a different velocity gradient $\nabla\mathbf{v}$ on either side of this plane. The jump of the velocity gradient can be represented by the dyadic product of the unit normal $\mathbf{n}$ of the discontinuity plane and a vector $\mathbf{g}$ defining the discontinuity mode of the velocity gradient, i.e.

$$[[\nabla\mathbf{v}]] = \mathbf{g} \otimes \mathbf{n} \neq \mathbf{0}. \tag{15}$$

Continuous equilibrium across the discontinuity requires (Rice and Rudnicki, 1980):

$$[[\dot{\mathbf{T}}]]\mathbf{n} = \mathbf{0}. \tag{16}$$

Herein the jump of the stress rate can be related to the jump of the Jaumann stress rate, i.e. $[[\dot{\mathbf{T}}]] = [[\overset{\circ}{\mathbf{T}}]] + [[\mathbf{W}]]\mathbf{T} - \mathbf{T}[[\mathbf{W}]]$, where $\mathbf{T}$ is the response of the hypoplastic model (11) and $\mathbf{W}$ denotes the antisymmetric part of the velocity gradient. Inserting the Jaumann stress rate into Eq. (16) leads to the relation:

$$f_s(\mathscr{L} : [[\mathbf{D}]])\mathbf{n} + \lambda f_s f_d(\mathscr{P} : \mathbf{N})\mathbf{n} + [[\mathbf{W}]]\mathbf{T}\mathbf{n} - \mathbf{T}[[\mathbf{W}]]\mathbf{n} = 0, \tag{17}$$

with $[[\mathbf{D}]] = [\mathbf{g} \otimes \mathbf{n} + \mathbf{n} \otimes \mathbf{g}]/2$, $[[\mathbf{W}]] = [\mathbf{g} \otimes \mathbf{n} - \mathbf{n} \otimes \mathbf{g}]/2$ and $\lambda = [[\sqrt{\mathbf{D} : \mathbf{D}}]]$. At the onset of shear banding the stress and the void ratio are the same on either side of the discontinuity plane. Thus, the quantities f_s, f_d,

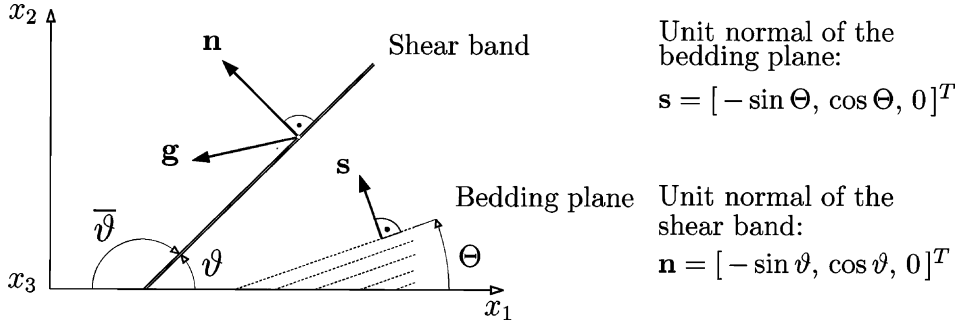

Fig. 8. Orientation of the bedding plane Θ and of the shear band ϑ and $\overline{\vartheta} = \Pi - \vartheta$.

$\mathscr{L}$, $\mathscr{P}$ and $\mathbf{N}$ are also the same and they are independent of the velocity gradient. It is a peculiarity in hypoplasticity that the possibility of different incremental stiffnesses due to a different velocity gradient on either side of the discontinuity is taken into account by the single relation (17) and there is no need to distinguish whether the material outside the shear band undergoes loading or unloading (e.g. Chambon and Desrues, 1985; Wu and Sikora, 1991; Bauer and Huang, 1997). Relation (17) can be rewritten as $\mathbf{Kg} = \lambda\mathbf{r}$ or

$$\mathbf{g} = \lambda\mathbf{K}^{-1}\mathbf{r}, \tag{18}$$

with $\mathbf{K} = f_s[\hat{a}^2(\mathbf{I} + \mathbf{n}\otimes\mathbf{n})/2 + (\hat{\mathbf{T}}(\mathbf{n}\otimes\mathbf{n}))\hat{\mathbf{T}}] + [(\mathbf{n}(\mathbf{T}\mathbf{n}))\mathbf{I} - (\mathbf{n}\otimes\mathbf{n})\mathbf{T} - \mathbf{T} + \mathbf{T}(\mathbf{n}\otimes\mathbf{n})]/2$, and $\mathbf{r} = -f_s f_d(\mathscr{P} : \mathbf{N})\mathbf{n}$. Inserting relation (18) for $\mathbf{g}$ into the norm of $[[\mathbf{D}]]$, i.e. $\sqrt{[[\mathbf{D}]] : [[\mathbf{D}]]} = \sqrt{[(\mathbf{gg}) + (\mathbf{gn})^2]/2} = \gamma$ leads to the bifurcation condition:

$$f(\vartheta) = \sqrt{\frac{(\mathbf{K}^{-1}\mathbf{r})(\mathbf{K}^{-1}\mathbf{r}) + ((\mathbf{K}^{-1}\mathbf{r})\mathbf{n})^2}{2}} - \frac{\gamma}{|\lambda|} = 0. \tag{19}$$

The components of the unit normal $\mathbf{n}$ of the discontinuity plane are related to the unknown shear band inclination angle ϑ, i.e. $\mathbf{n} = [-\sin\vartheta, \cos\vartheta, 0]^{\mathrm{T}}$ with respect to the co-ordinate system in Fig. 8. $\mathbf{K}$ and $\mathbf{r}$ depend on the current state quantities $(e, \mathbf{T})$ and on the inclination angle Θ of the bedding plane. In order to find the lowest possible bifurcation stress ratio the value of $\gamma/|\lambda|$ can be set equal to 1 (Wu and Sikora, 1992; Bauer, 1999). Thus, relation (19) represents an equation for the unknown ϑ, whereby only real solutions to (19) indicate the possibility of a shear band bifurcation.

In the following the bifurcation condition (19) is examined for stress paths which are related to homogeneous compression under plane strain conditions and a constant lateral pressure starting from an isotropic stress state (Fig. 9). The lowest bifurcation stress ratio obtained from the bifurcation analysis occurs before the peak state and it is marked by a dot. Therefore the solid curves in Fig. 9 denote states in which a spontaneous shear band bifurcation is not possible. But states above the first bifurcation point (dotted/dashed curves) again fulfill criterion (19) also for $\gamma > |\lambda|$ as discussed in detail for an inherently isotropic material by Bauer (1999). The lowest bifurcation stress ratio is higher for a lower bedding angle. Solutions to the bifurcation condition (19) are analyzed within $0° \leqslant \vartheta \leqslant 180°$ as shown in Fig. 10 for bedding angles of 0°, 30°, 60° and 90°. The analysis shows that for $\Theta = 0°$ and $\Theta = 90°$ (Fig. 10a, d) two shear band inclination angles ϑ are obtained at the same bifurcation stress state for $f(\vartheta) = 0$. The two

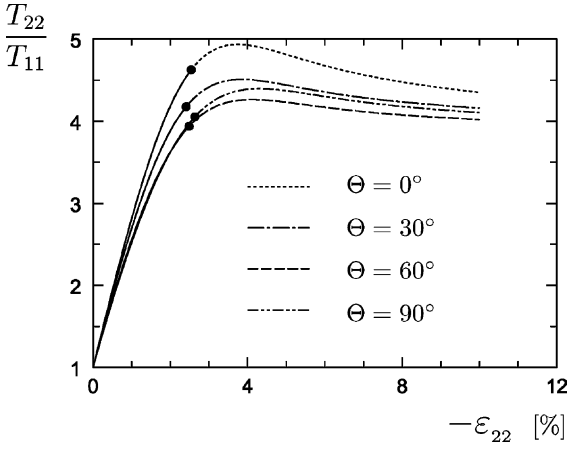

Fig. 9. Stress–strain relation and onset of shear band bifurcation for homogeneous compression under plane strain conditions and a constant lateral pressure $T_{11} = -100$ kPa, an initial void ratio $e_0 = 0.6$ and different bedding angles Θ.

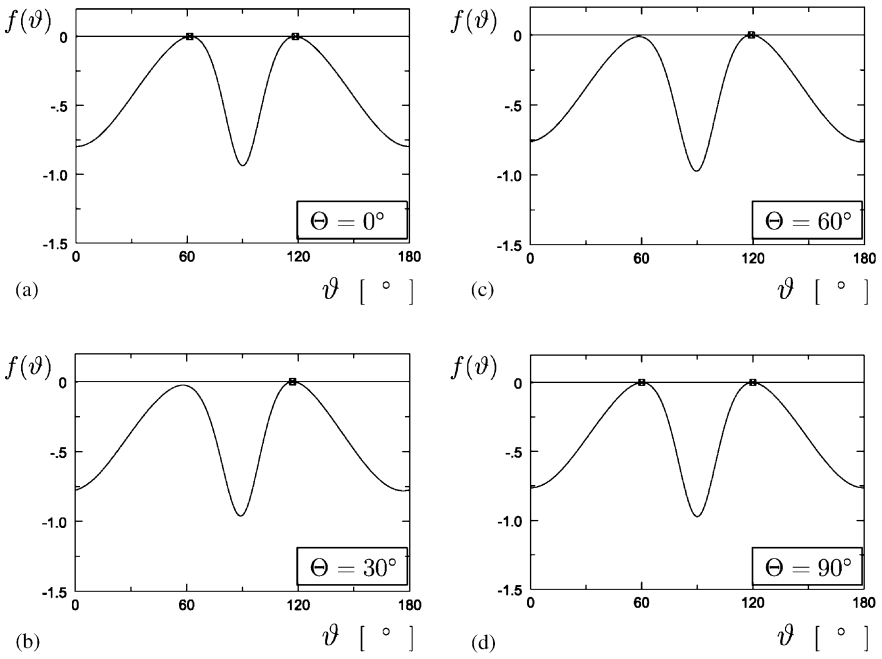

Fig. 10. Function $f(\vartheta)$ corresponds to bifurcation point for bedding angle: (a) $\Theta = 0°$, (b) $\Theta = 30°$, (c) $\Theta = 60°$, (d) $\Theta = 90°$.

possible shear bands are symmetric to the x_2-axis. However, within the range of $0° < \Theta < 90°$ only one single shear band is possible at the lowest bifurcation stress state and the corresponding shear band inclination angles ϑ are greater than 90°. The results in Fig. 10b and c show that the difference between the two peak values for $f(\vartheta)$ is very small, which indicates that a shear band within the range of $0° < \vartheta < 90°$ could also appear as a result of deviations from the ideal conditions assumed for the present investigation. Moreover, for states beyond the first bifurcation point more than one shear band is possible and also shear bands within the range of $0° < \vartheta < 90°$ will occur. In contrast to an isotropic material the inclination of the second shear band obtained for an anisotropic material is usually not symmetric to the x_2 axis as can be detected in Fig. 10b and c. The supplementary shear band inclination angle $\overline{\vartheta} = 180° - \vartheta$ versus the bedding angle Θ is represented in Fig. 11a. The predicted shear band inclination $\overline{\vartheta}$ has a maximum

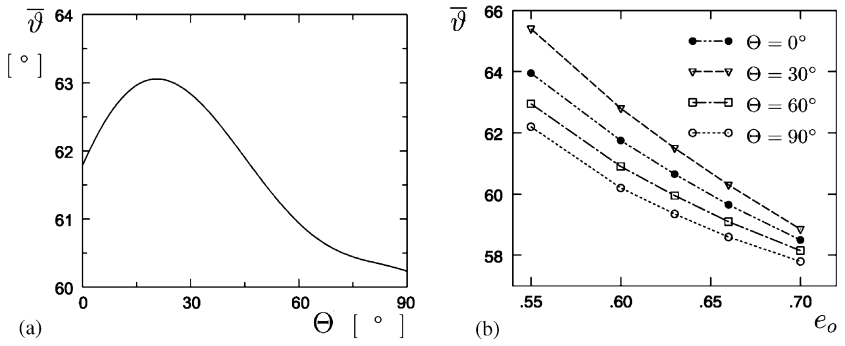

Fig. 11. (a) Supplementary inclination angle $\overline{\vartheta} = 180° - \vartheta$ versus bedding angle Θ, (b) shear band inclination $\overline{\vartheta}$ versus initial void ratio e_0.

for $\Theta \approx 20°$ while the minimum value is obtained for $\Theta = 90°$. The influence of the initial void ratio e_0 on the shear band inclination $\overline{\vartheta}$ is shown for various bedding angles Θ in Fig. 11b. The predicted shear band inclination is higher for a lower void ratio and decreases with an increase of the void ratio.

3.2. Influence of the off-axis loading on the shear band orientation

The bifurcation analysis carried out in the preceding section does not reflect the complete bifurcation and stability behavior of a standard biaxial compression test with a mixed control of the stress and displacement boundary conditions. For an anisotropic material the principal stresses and the principal strains are not usually coaxial so that the stress and void ratio distribution within a real specimen becomes inhomogeneous as a result of the off-axis loading. The off-axis loading can show a strong influence on the orientation of the shear band depending on the slenderness of the specimen as demonstrated in the following for two different sizes of rectangular samples: a slender sample with an initial width of 25 mm and a height of 100 mm, and a stout sample with an initial width of 50 mm and a height of 100 mm. For the finite element calculation the samples are discretized by quadratic elements with a length of 1.25 mm. The test is controlled by increasing the vertical displacement at the top parallel to the bottom. The horizontal movement of the top side and the bottom side is unrestricted with the exception of the center of the top side. On the vertical sides of the specimen the pressure is kept constant and the boundaries are free to move. For all calculations the same initially isotropic stress states of $T_0 = -100$ kPa and a bedding plane angle of $\Theta = 30°$ are assumed.

For the case of a slender specimen and an initially homogeneous void ratio of $e_0 = 0.6$ the distribution of the deviatoric strain rate and of the void ratio in the deformed configuration is shown in Fig. 12 for several vertical displacements. In particular the darker area in Fig. 12I means a higher deviatoric strain rate, while the brighter area in Fig. 12II means a higher void ratio as a result of dilatancy. The rectangular specimen assumes a skewed shape (S-shape) at a relatively low strain level. This is different from the result with an isotropic model, where the specimen keeps its rectangular shape up to a fairly high strain level (Bauer and Huang, 1997). The distortion of the anisotropic specimen is ascribed to the non-coaxiality between stress and strain rate. A closer examination of the expression $\mathscr{P}(\mathbf{S})$ in the constitutive equation (11) reveals that the stress and strain rates are coaxial only for the bedding angles of 0° and 90°. It should be noted that in the present finite element calculation the location of strain localization is triggered by the off-axis loading and no weak element is introduced to initiate the onset of strain localization. Thus, strain localization develops from the middle of the sample (Fig. 12.I.a). The orientation of intense strain localization right after the onset is greater than 90° as it is also obtained from the shear band bifurcation analysis in Section 3.1. However, with advanced vertical compression the area of intense strain localization jumps to an inclination angle of less than 90° as can be detected by comparing Fig. 12.I.a with Fig. 12.I.b, and the orientation of the final shear band lies within the same quadrant as the inclination of the bedding plane (Fig. 12.I.c).

While the deviatoric strain rate distribution is instantaneous, the corresponding contour plot of the void ratio is cumulative and represents the deformation history within the sample (Fig. 12.II.a–c). It is clearly visible that the zone of strain localization in Fig. 12.I.c is smaller than the band of higher void ratios in Fig. 13.II.c. This suggests that the distribution of the void ratio does not clearly permit an unequivocal identification of the active thickness of the shear band. In this context it is worth noting that the present finite element calculation is more of a qualitative than quantitative nature because the thickness of the localized zone depends on the size of the finite element. This shortcoming of classical continuum models can be overcome for instance by an extension of the constitutive model to a Cosserat continuum as proposed for an isotropic hypoplastic material model by Tejchman and Bauer (1996), Tejchman (1997), Tejchman and Gudehus (2001), Huang et al. (2002), and Huang and Bauer (2003).

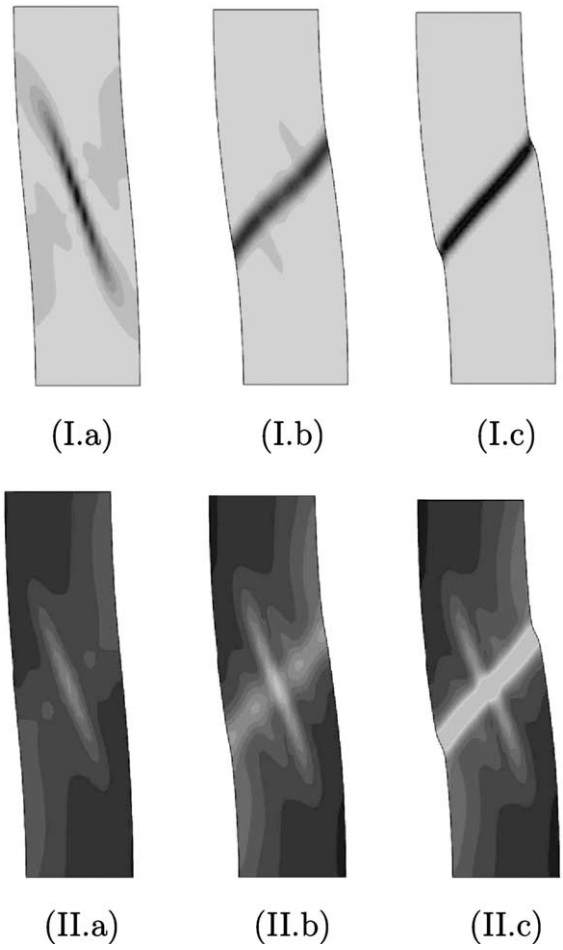

Fig. 12. Biaxial compression of a slender sample ($h/b = 4$) under a constant lateral pressure and an initially constant void ratio: (I) concentration of the deviatoric strain rate and (II) contour plot of the void ratio for a vertical displacement of: (a) 5 mm, (b) 6 mm and (c) 7 mm.

In order to investigate the sensitivity of the shear band orientation with respect to the fluctuation of the initial density a finite element calculation with a probabilistic distribution of the initial void ratio was performed. Herein the probabilistic distribution of the void ratio is modeled in the same way as proposed by Shahinpoor (1981) and applied to finite element calculations by Nübel (1998). The results obtained for the slender sample are shown in Fig. 13.

A comparison of Fig. 12 with Fig. 13 at a low strain level shows that the skewed specimen shape (Fig. 12) cannot be observed in Fig. 13. It seems that the distortion of the specimen is suppressed by the probabilistic void ratio. This interesting phenomenon deserves further investigation. Furthermore, a crossed band pattern with intense strain localization can be observed in the same configuration (Fig. 13.I.a and I.b), while only one single band is dominant in the case of an initially constant void ratio (Fig. 12.I.a). With advanced vertical compression strain localization continues to localize only within a single band in both cases (Fig. 12.I.c and Fig. 13.I.c). The location of the final band is influenced by the probability distribution of the initial void ratio. However, the inclination of the shear band is the same in both cases with homogeneously and probabilistically distributed void ratios.

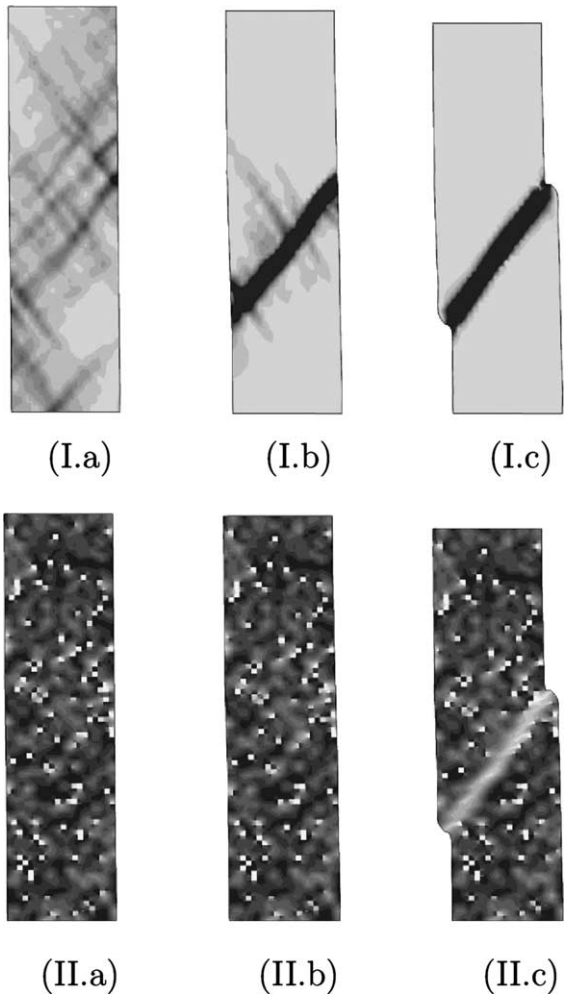

Fig. 13. Biaxial compression of a slender sample ($h/b = 4$) under constant lateral pressure and probabilistic distribution of the initial void ratio: (I) concentration of the deviatoric strain rate and (II) contour plot of the void ratio for a vertical displacement of: (a) 3.5 mm, (b) 4 mm and (c) 7 mm.

The influence of the size of the sample on the final orientation of the shear band is shown in Fig. 14 for a stout sample with a probabilistic distribution of the initial void ratio. As the inclination of the specimen remains small, the off-axis loading is not significant so that the inclination of strain localization at the lowest possible stress state becomes dominant. Thus, the ratio of the height to the width of the sample determines the off-axis loading and consequently influences the orientation of the final shear band.

4. Conclusions

The present paper treats initial and induced anisotropy in a unified way. The initial anisotropy is accounted for by a structure tensor, which is defined by the dyadic product of the normal vector of the isotropic plane. In order to account for the influence of particle rotation at the microscopic level the

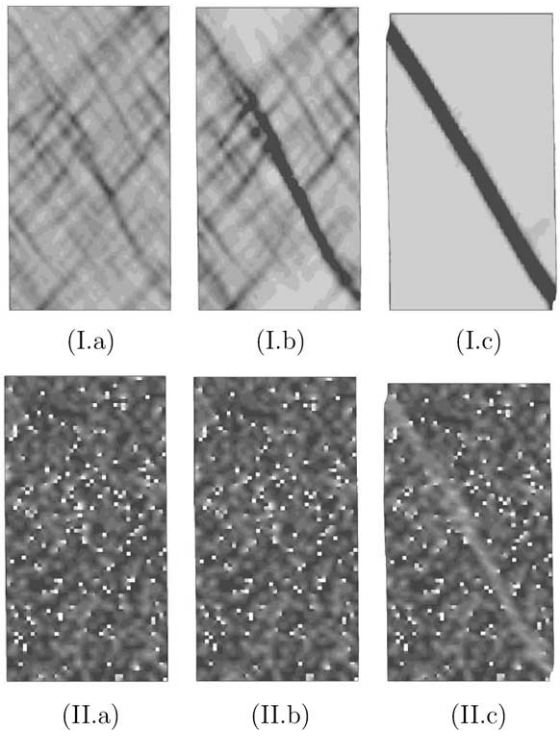

Fig. 14. Biaxial compression of a stout sample ($h/b = 2$) under constant lateral pressure and probabilistic distribution of the initial void ratio: (I) concentration of the deviatoric strain rate and (II) contour plot of the void ratio for a vertical displacement of: (a) 4 mm, (b) 4.5 mm and (c) 7 mm.

coefficients of the tensorial function are allowed to evolve. It is assumed that for large shearing the influence of anisotropy declines and the stress ratio and the volume strain tend towards a stationary state which is independent of the initial state.

The effect of initial anisotropy on shear band formation is investigated by analytical and numerical methods. The analytical results show that shear banding is strongly influenced by the stress state, the current void ratio and the orientation of the bedding plane. At the lowest bifurcation stress ratio only a single shear band is possible with the exception of loading parallel or perpendicular to the direction of the bedding plane, where two symmetric shear bands appear. The inclination of the shear band is higher for lower void ratios and lower bedding angles. In the case of a slender sample the results of the numerical simulations of plane strain compression tests show a jump from a steep shear band to a flat shear band with increasing axial displacement. Thus the orientation of shear strain localization obtained from the analytical bifurcation analysis is different from the orientation detected under larger deformation. Since the analytical solution deals with one single element under uniform stress, the shear band orientation may deviate from that appearing in a full boundary value problem. The distribution of the deviatoric strain rate and the void ratio justifies distinguishing between the active thickness of the shear band in the current configuration and the shear band thickness related to the history of shear dilatancy which is manifested by a higher void ratio. The calculations with an initially probabilistic void ratio distribution show numerous potential shear bands at low strain level. With increasing deformation a dominant shear band emerges out of the numerous potential shear bands. The latter is thought to be particularly relevant for progressive failure in natural sand deposits, where the void ratios also vary within a wide range.

The present paper is a first attempt in the numerical investigation of shear band formation in anisotropic sand. The result on shear band thickness is only indicative, since the underlying constitutive model does not possess a characteristic length. However, the constitutive equation can be readily extended to incorporate a characteristic length via the Cosserat continuum. Nevertheless the main outcomes of the present paper will remain valid.

References

Arthur, J.R.F., Phillips, A.B., 1975. Homogeneous and layered sand in triaxial compression. Géotechnique 25 (4), 799–815.

Bauer, E., Wu, W., 1994. Extension of hypoplastic constitutive model with respect to cohesive powders. In: Siriwardane, Zaman, (Eds.), Proceedings of the Eighth International Conference on Computer Methods and Advances in Geomechanics, IACMAG 94. Balkema Press, pp. 531–536.

Bauer, E., 1995. Constitutive modelling of critical states in hypoplasticity. In: Pande, Pietruszczak, (Eds.), Proceedings of the Fifth International Symposium on Numerical Models in Geomechanics. Balkema Press, pp. 15–20.

Bauer, E., 1996. Calibration of a comprehensive hypoplastic model for granular materials. Soils and Foundations 36 (1), 13–26.

Bauer, E., Huang, W., 1997. The dependence of shear banding on pressure and density in hypoplasticity. In: Adachi, Oka, Yashima, (Eds.), Proceedings of the 4th International Workshop on Localisation and Bifurcation Theory for Soils and Rocks, 1998. Balkema Press, pp. 81–90.

Bauer, E., Huang, W., 1999. Effect of initial anisotropy on shear banding in granular materials. In: Pande, Pietruszczak, Schweiger, (Eds.), Proceedings of the 7th International Symposium on Numerical Models in Geomechanics. Balkema Press, pp. 121–126.

Bauer, E., 1999. Analysis of shear band bifurcation with a hypoplastic model for a pressure and density sensitive granular material. Mechanics of Materials 31, 597–609.

Bauer, E., 2000. Conditions for embedding Casagrande's critical states into hypoplasticity. Mechanics of Cohesive-Frictional Materials 5, 125–148.

Bauer, E., Herle, I., 2000. Stationary states in hypoplasticity. In: Kolymbas, (Ed.), Constitutive Modelling of Granular Materials. Springer-Verlag, pp. 167–192.

Bauer, E., Wu, W., Huang, W., 2003. Influence of initially transverse isotropy on shear banding in granular materials. In: Labuz, J.F., Drescher, A. (Eds.), Proceedings of the International Workshop on Bifurcation and Instabilities in Geomechanics, Minneapolis, Minnesota, 2002. Balkema Press, pp. 161–172.

Boehler, J.P., Sawczuk, A., 1977. On yielding of oriented solids. Acta Mechanica 27, 185–206.

Chambon, R., Desrues, J., 1985. Bifurcation par localisation et non linéarité incrémentale: un exemple heuristique d'analyse compléte. Plastic Instability, Presses de l'ENPC ed., Paris, pp. 101–113.

Chambon, R., 1989. Bases théoriques d'une loi de comportement incrémentale consistante pour les sols. Groupe C.O.S.M. Rapport de Recherche.

Charlier, R., Chambon, R., Desrues, J., Hammad, W., 1991. Shear band bifurcation and soil modeling: a rate type constitutive law for explicit localization analysis. In: Desai, Krempl, (Eds.), 3rd International Conference on Constitutive Laws for Engineering Materials, Tucson, 1991. ASME Press, pp. 1–4.

Darve, F., 1974. Contribution à la détermination de la loi rhéologues incrémentale des sols. Thése de docteur-ingénieur Université Scientifique et Médicale de Grenoble, France.

Darve, F., 1991. Incrementally non-linear constitutive relationships. In: Darve, (Ed.), Geomaterials: Constitutive Equations and Modelling. Elsevier Press, pp. 213–237.

Desrues, J., Chambon, R., 2002. Shear band analysis and shear moduli calibration. International Journal of Solids and Structures 39, 3757–3776.

Gudehus, G., 1996. A comprehensive constitutive equation for granular materials. Soils and Foundations 36 (1), 1–12.

Herle, I., Gudehus, G., 1999. Determination of parameters of a hypoplastic constitutive model from properties of grain assemblies. Mechanics of Cohesive-Frictional Materials 4, 461–486.

Hill, R.J., 1962. Acceleration waves in solids. J. Mech. Phys. Solids (10), 1–16.

Huang, W., 2000. Hypoplastic modelling of shear localisation in granular materials. Doctoral Thesis, Graz University of Technology.

Huang, W., Nübel, K., Bauer, E., 2002. Polar extension of a hypoplastic model for granular materials with shear localization. Mechanics of Materials 34, 563–576.

Huang, W., Bauer, E., 2003. Numerical investigations of shear localization in a micro-polar hypoplastic material. International Journal for Numerical Anal. Methods Geomechanics 27, 325–352.

Kolymbas, D., 1985. A generalized hypoelastic constitutive law. Proc. XIth ICSMFE 5, p. 2626.

Kolymbas, D., 1991. An outline of hypoplasticity. Archive of Applied Mechanics 3, 143–151.

Lam, W.K., Tatsuoka, F., 1988. Effect of initial anisotropic fabric and σ_2 on strength and deformation characteristics of sand. Soils and Foundations 28 (1), 89–106.

Matsuoka, H., Nakai, T., 1977. Stress–strain relationship of soil based on the 'SMP'. In: Proc. of Speciality Session 9, IX Int. Conf. Soil Mech. Found. Eng., Tokyo, pp. 153–162.

Nagtegaal, J.C., Parks, D.M., Rice, J.R., 1974. On numerically accurate finite element solutions in fully plastic range. Computer Methods in Applied Mechanics and Engineering 4, 153–177.

Nübel, K., Karcher, C., 1998. FE simulations of granular material with a given frequency distribution of voids as initial condition. Granular Matter 3, 1005–1112.

Oda, M., Nemat-Nasser, S., Konishi, J., 1985. Stress induced anisotropy in granular masses. Soil and Foundations 25 (3), 85–97.

Rice, J., Rudnicki, J.W., 1980. A note on some features on the theory of localization of deformation. International Journal of Solids and Structures 16, 597–605.

Roddeman, D., 1997. FEM-Implementation of Hypoplasticity. Internal Report of the Institute of Geotechnical and Tunnel Engineering. University of Innsbruck, Austria.

Rudnicki, J.W., Rice, J., 1975. Conditions for the localization of deformation in pressure sensitive dilatant materials. J. Mech. Phys. Solids 23, 371–394.

Shahinpoor, M., 1981. Statistical mechanical considerations on storing bulk solids. Bulk Soils Handling 1.

Tamagnini, C., Viggiani, G., Chambon, R., 2000. A review of two different approaches to hypoplasticity. In: Kolymbas, (Ed.), Constitutive Modelling of Granular Materials. Springer Press, pp. 107–145.

Tamagnini, C., Viggiani, G., Chambon, R., 2001. Some remarks on shear band analysis in hypoplasticity. In: Mühlhaus, Dyskin, Pasternak, (Eds.), 5th International Workshop on Localisation and Bifurcation Theory in Geomechanics, Perth, 1999. Balkema Publisher, pp. 85–93.

Tatsuoka, F., Nakamura, S., Huang, C., Tani, K., 1990. Strength anisotropy and shear band direction in plane strain tests of sand. Soils and Foundations 30 (1), 35–54.

Tejchman, J., Bauer, E., 1996. Numerical simulation of shear band formation with a polar hypoplastic constitutive model. Computers and Geotechnics 19 (3), 221–244.

Tejchman, J., 1997. Modelling of shear localisation and autogeneous dynamic effects in granular bodies. Veröffentlichungen des Institutes für Bodenmechanik und Felsmechanik der Universität Fridericiana in Karlsruhe, Heft 140.

Tejchman, J., Gudehus, G., 2001. Shearing of a narrow granular layer with polar quantities. International Journal of Numerical Methods Geomech. 25, 1–28.

Truesdell, C., 1955. Hypoelasticity. J. Rat. Mech. Anal. 4, 83–133.

Wu, W., 1998. Rational approach to anisotropy of sand. International Journal of Numerical Anal. Methods Geomech. 22, 921–940.

Wu, W., 2000. Nonlinear analysis of shear band formation in sand. International Journal of Numerical Anal. Methods Geomech. 24, 245–263.

Wu, W., Bauer, E., 1992. A hypoplastic model for barotropy and pyknotropy of granular soils. In: Kolymbas, (Ed.), Proceedings of the International Workshop on Modern Approaches to Plasticity, 1993. Elsevier, pp. 225–245.

Wu, W., Kolymbas, D., 1990. Numerical testing of the stability criterion for hypoplastic constitutive equations. Mechanics of Materials 9, 245–253.

Wu, W., Kolymbas, D., 2000. Hypoplasticity then and now. In: Kolymbas, (Ed.), Constitutive Modelling of Granular Materials. Springer Press, pp. 57–105.

Wu, W., Sikora, Z., 1991. Localized bifurcation in hypoplasticity. International Journal of Engineering Science 29 (2), 195–201.

Wu, W., Sikora, Z., 1992. Localized bifurcation in pressure sensitive dilatant granular materials. Mechanical Research Communications 19, 289–299.

Wu, W., Bauer, E., Kolymbas, D., 1996. Hypoplastic constitutive model with critical state for granular materials. Mechanics of Materials 23, 45–69.

Yamada, Y., Ishihara, K., 1979. Anisotropic deformation characteristics of sand under three dimensional stress conditions. Soils and Foundations 19 (2), 79–94.